

HOW STRANGE IS THE PROTON?*

PIOTR DECOWSKI

Smith College, Northampton, MA 01063, USA

(Received November 15, 2005)

The paper discusses application of parity violating polarized electron scattering off nucleons to study strange form factors of the nucleon. The results from the recent HAPPEX experiment are discussed in more detail.

PACS numbers: 11.30.Er, 13.40.Gp, 13.60.Fz, 14.20.Dh

1. Introduction

As for today we are still missing the theory able to describe the nucleon structure in a consistent way at low and high momentum transfers. At small Q^2 (length scale comparable with the nucleon size) hadron properties are explained by the Quark Model in terms of the three massive constituent quarks. At smaller distances probed by higher Q^2 hadron structure reveals a pattern of weakly interacting gluons, nearly mass-less current quarks and the sea of virtual quark/anti-quark pairs (see Fig. 1). It is the region in which the perturbative QCD works well. A smooth connection between these two approaches is not established yet. The difficulty in reuniting both approaches is referred to as the “quark–hadron duality” problem.

Investigations of strange quark contributions to the nucleon electromagnetic properties can help to understand this duality. Strange quarks as the second lightest are abundant and unique exponents of the sea because, in contrast to the up and down quarks, there are no valence strange quarks. At small Q^2 they represent the sea over distances relevant to the Quark Model. Explicit knowledge of the sea at such large distances is important in view of the quark–hadron duality. In addition, strange quarks can help to answer the question how much the different flavors of quarks contribute to the low-energy properties of the nucleon.

* Presented at the XXIX Mazurian Lakes Conference on Physics
August 30–September 6, 2005, Piaski, Poland.

Earlier experiments had shown that the contributions of strange quarks to static properties of the nucleon can be significant. Analysis of the πN scattering, though the subject of huge theoretical uncertainties, suggest that the strange quark contribution to the nucleon mass $\langle N|\bar{s}s|N\rangle$ could be as large as 23% [1]. The strange quark contribution to the proton spin $\langle N|\bar{s}\gamma_\mu\gamma^5s|N\rangle = 2(\Delta s)s_\mu$, obtained from the next-to-leading order perturbative QCD analysis of the world data on polarized electron deep inelastic scattering off polarized targets, is $\Delta s = -0.045 \pm 0.007$ [2] which is surprisingly large considering that the contribution of all quarks to the proton spin $\Delta\Sigma = \Delta u + \Delta d + \Delta s$ is only ~ 0.25 . On the other hand the muon tagged $\nu_\mu N$ and $\bar{\nu}_\mu N$ reactions provide information that the strange quarks and anti-quarks share only $\int_0^1 x(\bar{s} + s) dx \approx 2\%$ of the nucleon momentum [3].

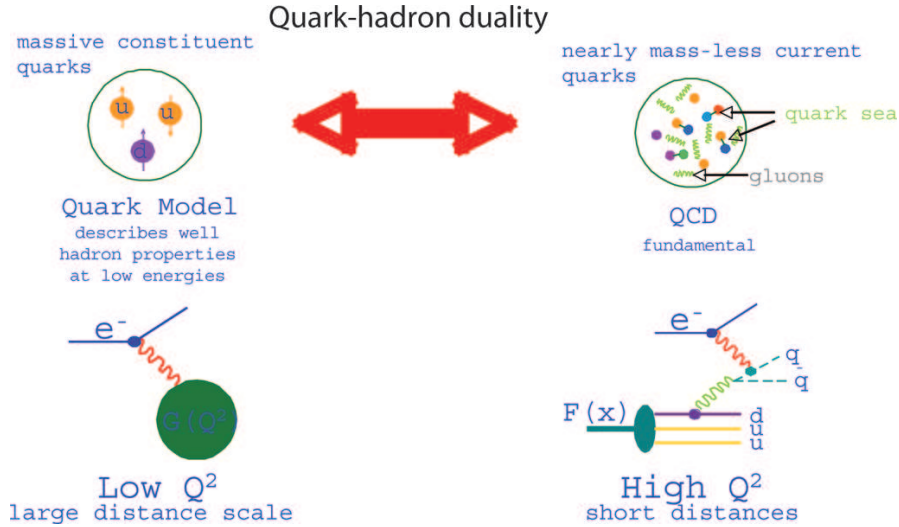


Fig. 1. Quark-hadron duality. At large distance scale nucleon is described by the Quark Model of three massive constituent quarks yielding the nucleon electromagnetic form factors $G(Q^2)$. At short distances hadron reveals rich structure of gluons and almost mass-less quarks/anti-quarks with distributions $F(x)$ depending on Bjorken variable x .

The strange quark vector current $\langle N|\bar{s}\gamma_\mu s|N\rangle$ can be conveniently measured by parity violating longitudinally polarized electron scattering off the nucleon (see *e.g.* [4]). In this process the parity conserving photon exchange interferes with the parity violating weak interaction mediated by the Z^0 boson (see Fig. 2). The amplitude related to the Z^0 exchange is a small

fraction $\sim Q^2/M_Z^2$ of the total amplitude and is not visible in the scattering cross section. However, it can be extracted from the small asymmetry in scattering of the longitudinally polarized electrons:

$$A^{\text{PV}} = \frac{\sigma^{\text{R}} - \sigma^{\text{L}}}{\sigma^{\text{R}} + \sigma^{\text{L}}} = \frac{|f^{\text{R}}|^2 - |f^{\text{L}}|^2}{|f^{\text{R}}|^2 + |f^{\text{L}}|^2} \approx \frac{f_Z^{\text{R}} - f_Z^{\text{L}}}{f_\gamma} \sim \frac{Q^2}{M_Z^2} \sim 10^{-4} - 10^{-6}, \quad (1.1)$$

where σ^{R} and σ^{L} are cross sections for the right- and left-handed electrons, respectively, with corresponding scattering amplitudes f^{R} and f^{L} . The amplitudes f_γ and f_Z probe nucleon structure with different weights determined by the electromagnetic and the weak charges of the constituent quarks. This fact makes possible extraction of the strange quarks contribution to the nucleon charge and magnetization.

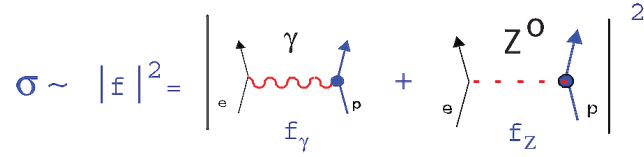


Fig. 2. In electron scattering the scattering amplitude is a sum of parity conserving term describing the photon exchange and small parity violating term related to the exchange of heavy Z^0 boson.

2. Parity violation in the $\vec{e}P$ scattering

Table I lists electromagnetic and weak charges of electrons and quarks in terms of the Weinberg angle θ_W . At forward angles the asymmetry A^{PV} is proportional to the product of electron axial (g_Z^{A}) and target vector (g_Z^{V}) weak charges (because the target is unpolarized). At backward angles the conservation of electron helicity induces target spin flip which results in an additional contribution of the target axial weak charge (and, correspondingly, the electron vector weak charge). The weak vector charges of d and s quarks are almost double of the u quark weak charge, whereas the opposite is true for the electromagnetic charges.

For the scattering off proton

$$A^{\text{PV}} = \frac{\sigma^{\text{R}} - \sigma^{\text{L}}}{\sigma^{\text{R}} + \sigma^{\text{L}}} = -\frac{G_{\text{F}}Q^2}{\pi\alpha\sqrt{2}} \left\{ \frac{\varepsilon G_{\text{E}}^{p\gamma} G_{\text{E}}^{pZ} + \tau G_{\text{M}}^{p\gamma} G_{\text{M}}^{pZ}}{\varepsilon(G_{\text{E}}^{p\gamma})^2 + \tau(G_{\text{M}}^{p\gamma})^2} - \frac{2\left(\frac{1}{4} - \sin^2\theta_W\right)\sqrt{\tau(1+\tau)}\sqrt{1-\varepsilon^2} G_{\text{M}}^{p\gamma} G_{\text{A}}^{pZ}}{\varepsilon(G_{\text{E}}^{p\gamma})^2 + \tau(G_{\text{M}}^{p\gamma})^2} \right\}, \quad (2.1)$$

where $G_{E,M}^{\gamma,Z}$ are the electromagnetic and weak form factors, respectively, G_F is the Fermi constant, $\varepsilon = 1/(1 + 2(1 + \tau) \tan^2 \frac{\theta}{2})$ decreases from 1 to 0 with increasing scattering angle θ , and $\tau = Q^2/(4M_p^2)$.

TABLE I

Couplings of γ (q_{EM}) and Z^0 (g_Z) to electrons and quarks.

Particle	q_{EM}	g_Z^R	g_Z^L
e^-	-1	$\sin^2 \theta_W \approx 0.23$	$-1/2 + \sin^2 \theta_W \approx -0.27$
u	+2/3	$-2/3(\sin^2 \theta_W) \approx -0.15$	$1/2 - 2/3(\sin^2 \theta_W) \approx 0.35$
d, s	-1/3	$1/3(\sin^2 \theta_W) \approx 0.08$	$-1/2 + 1/3(\sin^2 \theta_W) \approx -0.42$
Particle	q_{EM}	$g_Z^V = 1/2(g_Z^R + g_Z^L)$	$g_Z^A = 1/2(g_Z^R - g_Z^L)$
e^-	-1	$-1/4 + \sin^2 \theta_W \approx -0.02$	1/4
u	+2/3	$1/4 - 2/3(\sin^2 \theta_W) \approx 0.10$	-1/4
d, s	-1/3	$-1/4 + 1/3(\sin^2 \theta_W) \approx -0.17$	1/4

The nucleon form factors can be expressed in terms of the quark flavor distributions weighted by the appropriate electromagnetic and weak charges:

$$\begin{aligned} G_{E,M}^{p\gamma} &= q_{EM}^u G_{E,M}^u + q_{EM}^d (G_{E,M}^d + G_{E,M}^s) \\ &= \frac{2}{3} G_{E,M}^u - \frac{1}{3} (G_{E,M}^d + G_{E,M}^s), \end{aligned} \quad (2.2)$$

$$\begin{aligned} G_{E,M}^{pZ} &= g_Z^{Vu} G_{E,M}^u + g_Z^{Vd} (G_{E,M}^d + G_{E,M}^s) \\ &= \left(\frac{1}{4} - \frac{2}{3} \sin^2 \theta_W\right) G_{E,M}^u - \left(\frac{1}{4} - \frac{1}{3} \sin^2 \theta_W\right) (G_{E,M}^d + G_{E,M}^s). \end{aligned} \quad (2.3)$$

On the other hand, the p - n isospin symmetry imposes that d , u distributions in the neutron are the same as, respectively, u , d distributions in the proton, thus

$$G_{E,M}^{n\gamma} = \frac{2}{3} G_{E,M}^d - \frac{1}{3} (G_{E,M}^u + G_{E,M}^s). \quad (2.4)$$

Equations (2.2), (2.3) and (2.4) allow to substitute the form factors $G_{E(M)}^u$ and $G_{E(M)}^d$ in the $G_{E(M)}^{pZ}$ by the known form factors $G_{E(M)}^{p\gamma}$ and $G_{E(M)}^{n\gamma}$, and by the strange form factor $G_{E(M)}^s$. For the proton it yields:

$$\begin{aligned} A^{PV} &= -\frac{G_F Q^2}{4\pi\alpha\sqrt{2}} \left\{ (1 - 4\sin^2 \theta_W) - \frac{G_E^n + \eta G_M^n + G_E^s + \eta G_M^s}{G_E^p + \eta G_M^p} \right. \\ &\quad \left. - \frac{2\sqrt{\tau(1+\tau)}\sqrt{1-\varepsilon} (1 - 4\sin^2 \theta_W) G_M^p G_A^{pZ}}{\varepsilon(G_E^p)^2 + \tau(G_M^p)^2} \right\}, \end{aligned} \quad (2.5)$$

where $\eta = \tau G_M^p / \varepsilon G_E^p$.

At forward angles the last term in the Eq. (2.5) containing the neutral weak axial form factor G_A^{pZ} is small because of the $\sqrt{1-\varepsilon}$ factor and can be neglected. Thus at forward angles

$$A_{\text{exp}}^{\text{PV}} = A_0^{\text{PV}} + A_s^{\text{PV}}, \quad (2.6)$$

where A_0^{PV} is asymmetry calculated from the known proton electromagnetic factors without taking into account the strange quarks. The strange contribution to the asymmetry appears in the form of combination $G_E^s + \eta G_M^s$ and only compilation of experiments at different kinematic conditions (different η 's) allow to separate strange electric and magnetic form factors.

At $Q^2=0$, because of the zero net strangeness in the proton, $G_E^s(Q^2=0) = 0$ whereas $G_M^s(Q^2=0) \equiv \mu_s$ gives strange contribution to the proton magnetic moment. The slope

$$\left. \frac{dG_E^s}{d\tau} \right|_{\tau=0} = -\frac{2}{3} M_p^2 \langle r_s^2 \rangle - \mu_s \equiv \rho_s$$

defines the strangeness Dirac rms radius $\langle r_s^2 \rangle$ (nonzero value of $\langle r_s^2 \rangle$ indicates that in the nucleon the strange quarks have different distribution than the strange anti-quarks; when $\langle r_s^2 \rangle$ is positive there are more strange quarks at larger radii).

There are a number of theoretical attempts aimed at calculating strange properties of the nucleon. They can be grouped in three broad categories: lattice QCD, hadronic models and effective hadronic theories (chiral perturbation theory, dispersion relations, *etc.*), see [5,6]. Predictions for μ_s and ρ_s vary very much, especially for the latter quantity for which the theoretical values range from ~ -6 to ~ 3 . Most calculations favor negative values of μ_s , either very small or between -0.2 and $-0.4 \mu_N$. This situation emphasizes need of experimental data to differentiate between existing theoretical models.

3. Experiments

As was discussed in the previous section, the elastic electroweak electron scattering off hydrogen target at forward angles provides $G_E^s + \eta(Q^2)G_M^s$, where η is determined by the reaction kinematics. At backward angles terms containing τ and $\sqrt{1-\varepsilon}$ dominate and a measurement at these angles provides combination of magnetic and axial form factors $G_M^s + \zeta(Q^2)G_A^Z$. Measurements at backward angles on deuterium target are sensitive mainly to G_A^Z because of the partial cancellation of proton and neutron magnetic moments in the spin-1 state. On the other hand the quasielastic scattering off the isoscalar helium target provides the G_E^s only.

Recently four groups published results of measurements of strange form factors. The SAMPLE Collaboration had run at MIT-Bates series of experiments at backward angles with liquid hydrogen and deuterium targets [7–9]. The HAPPEX Collaboration using CEBAF at TJNAL measured forward scattering off liquid hydrogen and cryogenic gas ^4He targets [10–12]. The A4 group at MAMI facility in Mainz published results from scattering at moderately forward angles off liquid hydrogen target [13–15]. The G0 Collaboration at TJNAL produced results covering broad Q^2 range thanks to the dedicated segmented detector which registered protons recoiling from the liquid hydrogen target at a range of angles [16]. Parameters of these experiments are summarized in Table II.

TABLE II

Experiments involved in measurement of the nucleon strange form factors.

Experiment	Location	Q^2 (GeV^2/c^2)	Form factors
SAMPLE	MIT-Bates	0.1	G_M^s
HAPPEX	TJNAF	0.5, 0.1	$G_E^s + 0.392G_M^s, G_E^s + 0.08G_M^s, G_E^s$
A4	MAMI, Mainz	0.23, 0.1	$G_E^s + 0.225G_M^s, G_E^s + 0.106G_M^s$
G0	TJNAF	0.12–1.0	$G_E^s + \eta(Q^2)G_M^s$

4. The HAPPEX experiment

The schematic overview of the HAPPEX experiment is shown in Fig. 3. Longitudinally polarized electrons ejected from the GeAs cathode by circularly polarized laser light were accelerated in the CEBAF to an energy of $\sim 3\text{ GeV}$. Pairs of opposite helicity windows lasting 33.3 ms each were created in a pseudo-random manner by applying high voltage pulse to the Pockels cell mounted in the laser beam. To minimize false asymmetries, the helicity of all pairs was periodically reversed in a passive way by insertion of a half-wave plate in the laser beam. The integrated flux of electrons scattered from the cryogenic target (liquid hydrogen or pressurized cold He gas) was measured in dedicated detectors installed in the focal planes of two high resolution magnetic spectrometers placed symmetrically on both sides of the beam. Intensity of the beam at the target (a few tens of micro-amperes) as well as its position, angle, and energy were closely controlled by the beam monitors at multiple locations to allow for removing from the measured asymmetries contributions induced by the helicity correlated asymmetries in the beam parameters.

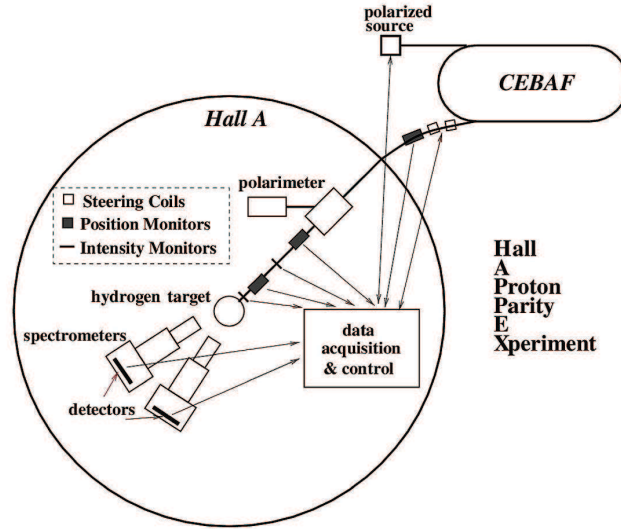


Fig. 3. Schematic overview of the HAPPEX experiment.

The HAPPEX experiment started in 1998. The subsequent runs took place in 1999, 2004, and in 2005 (currently in progress), each taking advantage from various improvements. Moving from bulk GaAs photocathode in 1998 to strained GaAs in 1999 to superlattice of doped GaAs layers in 2004 busted polarization of the electron beam from $\sim 38\%$ in 1998 to 86% in 2004. The auxiliary super-conducting septum magnets installed before the 2004 run in front of the magnetic spectrometers allowed to go down to the lower scattering angle of 6° , and consequently lower Q^2 (the minimal possible angle at which the magnetic spectrometers could be placed was 12.3°).

The expected asymmetry $A^{\text{PV}} \sim (1 - 10)$ parts per million (ppm) had to be measured with the precision < 1 ppm. The observed statistical fluctuations in one helicity window pair were ~ 1000 ppm. Thus measurement of $N > 1$ million pairs would reduce fluctuations to the desired level provided that the fluctuations indeed were purely statistical. To assure this, for each helicity window pair the measured detector asymmetry A_{det} had to be cleaned out from the beam induced helicity correlated asymmetries:

$$A_{\text{raw}} = A_{\text{det}} - A_Q - \sum_{i=1}^5 \beta_i \Delta x_i, \quad (4.1)$$

where A_Q is asymmetry in the beam intensity, Δx_i are asymmetries in the beam parameters (energy, x , y position, x , y angle), and β_i are sensitivities of the detector to the beam parameters (slopes in the detector response to

a given parameter change). These sensitivities were calibrated using two methods: regression, in which the natural beam jitter was used to measure the detector response, and beam modulation (dithering), in which the beam parameters were intentionally changed using steering coils in the beam line. Both methods produced similar results.

The statistical nature of the A_{raw} fluctuations is proved in Fig. 4 showing results from the 2004 run with the hydrogen target. The distribution is pure Gaussian over more than 5 orders of magnitude. The cumulative corrections due to the helicity correlated differences in beam parameters was about ~ 0.1 ppm in intensity, ~ 0.02 ppm in energy, ~ 7 nm in position, and ~ 4 nrad in angle. These numbers demonstrate good control of all the parameters and high stability of all the systems during the whole data taking period.

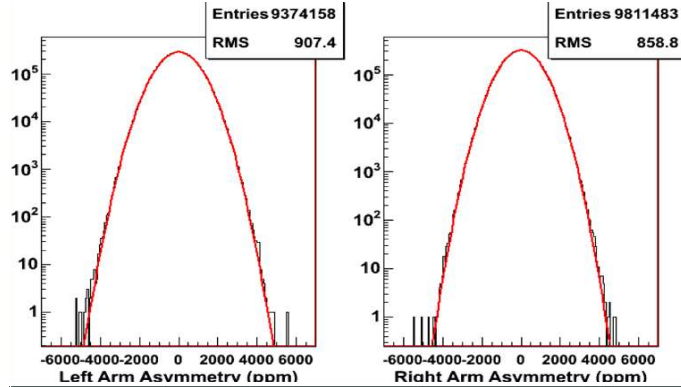


Fig. 4. Helicity window pair asymmetry A_{raw} in the left and the right spectrometers.

The physics asymmetry $A_{\text{exp}}^{\text{PV}}$ was obtained from A_{raw} by correcting for beam polarization, backgrounds, and finite acceptance:

$$A_{\text{exp}}^{\text{PV}} = \frac{K}{P_b} \frac{A_{\text{raw}} - \sum_i A_i f_i}{1 - \sum_i f_i}, \quad (4.2)$$

where P_b is the beam polarization, f_i , A_i are background fractions and their asymmetries, and K accounts for the range of kinematic acceptance.

The final values of asymmetries $A_{\text{exp}}^{\text{PV}}$ measured in the 2004 run are summarized in the Table III. The strange form factors are shown in Fig. 5 together with the world data [12]. The compilation of the data in Fig. 5 suggests a positive, nonzero value of G_M^s . This observation of the nonzero proton strange form factor is supported by the newly published G0 results shown in Fig. 6 [16]. The HAPPEX 2005 run, currently in progress, will provide results with significantly higher accuracy (see Fig. 7).

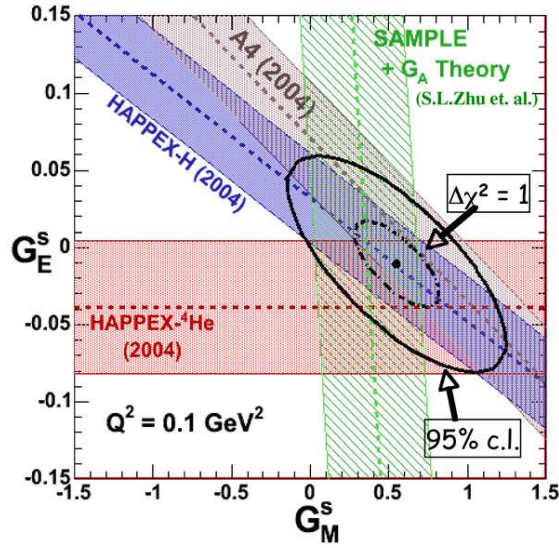


Fig. 5. Compilation of world data on strange form factors at $Q^2 = 0.1 \text{ (GeV/c)}^2$.

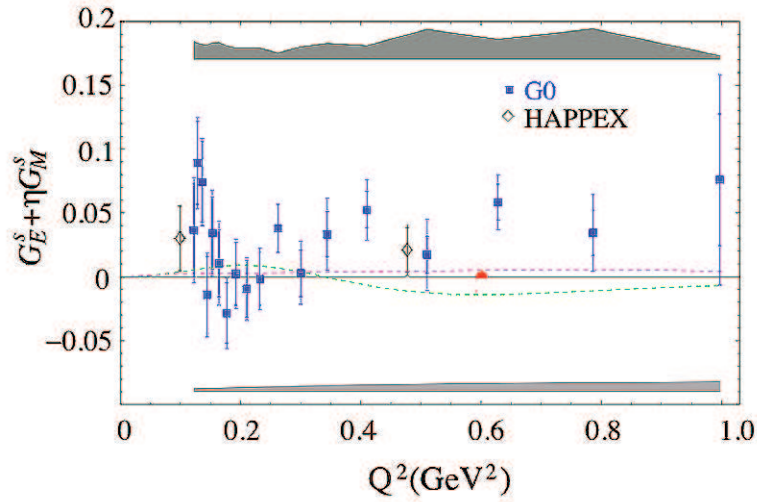


Fig. 6. Results from G0 experiment for the linear combination $G_E^s + \eta(Q^2)G_M^s$. For comparison also are shown HAPPEX results at $Q^2 = 0.5 \text{ GeV}^2$ and at $Q^2 = 0.1 \text{ GeV}^2$ (from the 2004 run).

TABLE III

Asymmetries measured in the 2004 HAPPEX run.

Target	20 cm LH ₂	20 cm ⁴ He gas ($T = 6.6$ K, ~ 20 atm)
E_{beam}, I	3.03 GeV, 35 μ A	3.03 GeV, 35 μ A
Scattering angle θ	6°	6°
Helicity pairs	11 million	3 million
$A_{\text{exp}}^{\text{PV}}$ (ppm)	-1.14 ± 0.24 (stat) ± 0.06 (sys)	6.72 ± 0.84 (stat) ± 0.21 (sys)
$A_0^{\text{PV}} (G^s = 0)$ (ppm)	-1.43 ± 0.11	7.483

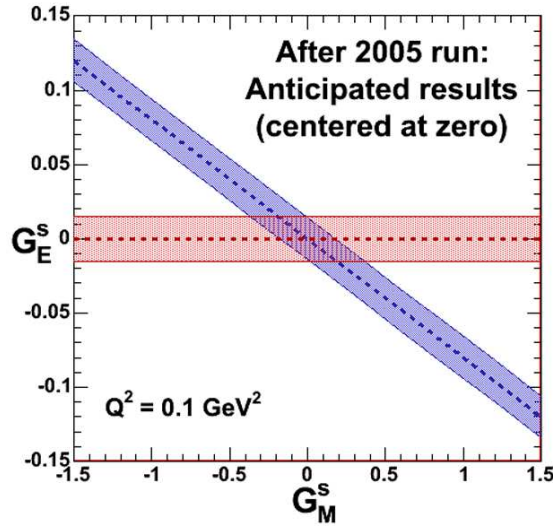


Fig. 7. Projected accuracy of the HAPPEX results after completion of taking data in 2005.

The author would like to thank HAPPEX Collaboration for discussions and provided information. This work was supported by the NSF RUI grant PHY0140267.

REFERENCES

- [1] M.M. Pavan *et al.*, *PiN Newslett.* **16**, 110 (2002).
- [2] E. Leader *et al.*, *Phys. Rev.* **D67**, 074017 (2003).
- [3] H.L. Lai *et al.*, *Phys. Rev.* **D55**, 1280 (1997).
- [4] K.S. Kumar, P.A. Souder, *Prog. Part. Nucl. Phys.* **45**, S333 (2000).
- [5] M.J. Musolf, [hep-ph/9712317](#).
- [6] P. Geiger, N. Isgur, *Phys. Rev.* **D55**, 299 (1997).
- [7] T. Ito *et al.*, *Phys. Rev. Lett.* **92**, 102003 (2004).
- [8] D.T. Spayde *et al.*, *Phys. Lett.* **B58**, 79 (2004).
- [9] E.J. Beise *et al.*, *Prog. Part. Nucl. Phys.* **54**, 289 (2005).
- [10] K.A. Aniol *et al.*, *Phys. Rev.* **C69**, 065501 (2004).
- [11] K.A. Aniol *et al.*, [nucl-ex/0506010](#), submitted to *Phys. Rev. Lett.*
- [12] K.A. Aniol *et al.*, [nucl-ex/0506011](#), submitted to *Phys. Rev. Lett.*
- [13] F.E. Mass *et al.*, *Phys. Rev. Lett.* **93**, 022002 (2004).
- [14] F.E. Mass *et al.*, *Phys. Rev. Lett.* **94**, 152001 (2004).
- [15] F.E. Maas, *Prog. Part. Nucl. Phys.* **55**, 320 (2005).
- [16] D.S. Armstrong *et al.*, *Phys. Rev. Lett.* **95**, 09200 (2005).